Journal of Engineering Science and Technology
Special Issue on SOMCHE 2014 & RSCE 2014 Conference, January (2015) 1 - 10

THE APPLICATION OF MAGNESIUM FERRITE PHOTOCATALYST FOR PHOTO TREATMENT OF METHYLENE BLUE

Zi Y. Kong[1], Nyap X. Wong[1], Sin W. Lum[1], Sze Y. Tan[1], Maksudur R. Khan[1], Chin K. Cheng[1,2,*]

[1]Faculty of Chemical & Natural Resources Engineering
[2]Rare Earth Research Centre
Universiti Malaysia Pahang, Lebuhraya Tun Razak, 26300 Gambang, Pahang , Malaysia
*Corresponding Author: chinkui@ump.edu.my

Abstract

The current work reports on the use of photocatalysis technique to decompose Methylene Blue (MB), an industrial-grade dye. Visible light-activated $MgFe_2O_4$ photocatalyst was synthesized using solid-solid method in a Mg:Fe ratio of 1:2 by mol. The photocatalyst was characterized using X-ray diffraction method (XRD) and field-emission scanning electron microscopy/energy dispersive x-ray analysis (FESEM-EDX). The results indicate that the solid catalyst exhibited high crystallinity with $MgFe_2O_4$ as the main compound. In addition, it has macropores structure with uniform formation of particles as suggested by FESEM images. Significantly, the performance and kinetics of photo-degradation of 20 ppm MB solution were studied over different catalyst loadings viz. 0.2, 0.5, 1.0, 1.5 and 2.0 g/L in the presence of xenon lamp (250 W). Kinetic modelling results indicate that the photodegradation followed the zero-order rate of reaction. Moreover, MB degradation seems to increase incrementally up to the 1.5 g/L beyond which the performance has deteriorated.

Keywords: Photocatalyst, Methylene blue, $MgFe_2O_4$, Visible light.

1. Introduction

The growing size of urban population, a rapid industrialization, an extreme dry-spell and indiscriminate discharge of organic pollutant (domestic, industry, plantation etc.) into water way have culminated in the shortage of potable water. Hence, pollution issue must be addressed immediately [1-4]. Today, one of the most common industrial effluents is synthetic colouring in the form of textile-

Nomenclatures

C_A	Concentration at time t, mg L^{-1}
C_{Ao}	Initial concentration, mg L^{-1}
k	apparent specific reaction rate, h^{-1}
t	Time, h

Greek Symbols

θ	Angle
λ	Cu Kα radiation

Abbreviations

BET	liquid N_2-physisorption
FESEM	field-emission scanning electron microscopy
MB	Methylene Biue
XRD	X-ray diffraction method

grade dyes; i.e., methylene blue (MB) is a highly water soluble organic dye [5]. The illegal dumping of MB is a common menace particularly in the developing countries. Therefore, an efficient and green catalytic decomposition of MB is clearly desirable. In this context, reduction of MB over the visible light-activated $MgFe_2O_4$ photocatalyst is an interesting subject and is the focus of the current investigation.

Photocatalysis is an area of reaction which employs light to activate a solid catalyst that in turns can increase the rate of a chemical reaction without itself being consumed. Among the various type of photocatalysts, titanium dioxide (TiO_2) is the most well known photocatalyst. Many of the past works centred on the development of TiO_2-based photocatalyst [6-10]. Unfortunately, TiO_2 has a wide band gap (> 3.1eV); hence only able to effectively capture the UV-light (200 to 400 nm), a 5% component of the solar energy spectrum compared to the visible light (anounted to 46%) [10-11]. Wen *et al.* (2009) proved that there was no obvious degradation of MB in the absence of TiO_2 catalyst under sunlight irradiation including UV and visible light. Sun *et al.* (2014) stated that unmodified TiO_2 showed about 10% MB removal, which was due to adsorption. Hence, development of new breed of photocatalysts is gaining pace. Specifically, a ferrite based catalyst can function under the visible light (400 to 700 nm), but details remained sketchy in particular when doped with the other metals such as magnesium.

Magnesium ferrite ($MgFe_2O_4$) is one of the ferrite-based photocatalysts that matches the aforementioned description owing to its stability in both acid-base and resistance towards photo-corrosion. In addition, it is non-toxic, possesses high chemical as well as photochemical stabilities [12]. In spinel structure, it can absorb visible light at about 2.0 eV due to its small band gap and less sensitive to the photo-anodic corrosion [10, 13-14]. This soft magnetic *n*-type semiconducting material has found a number of applications such as in heterogeneous catalysis, adsorption, sensors and also magnetic technologies [10, 15]. The $MgFe_2O_4$ is effective for the adsorption of SO_2 [16]. If they can be used as a photocatalyst as well as an adsorbing surface, it can make them highly effective in cleaning water sources by both the degradation of contaminants, as well as by removing other unwanted substances from the environment.

2. Experimental

2.1. Chemical and materials

Magnesium oxide (MgO) was from R&M Chemicals, Iron (III) oxide (Fe_2O_3) was purchased from Sigma Aldrich Chemical and the MB was procured from Fisher Scientific. All the chemicals were of analytical grade and used without further treatment.

2.2. Catalyst synthesis

Photocatalysts of different loadings were prepared using solid-solid method. The pre-calculated quantities of MgO and α-Fe_2O_3 were weighed and mixed thoroughly with deionized water. It was stirred for 3 h at room temperature before oven-dried at 353 K for 6 h. This procedure was followed by the air-calcination at 1173 K for 2 h. The calcined solid powder was then ground for characterization and reaction study.

2.3. Characterization technique

The synthesized photocatalysts were subjected to a series of characterization. The crystalline structure was identified using the Rigaku Miniflex II. The XRD measurement employed radiation, λ=1.5418Å at 30 kV and 15 mA from 2θ of 10^o to 80^o with a step size of 0.02^o and a step time of 1 s. In addition, the size and morphology of the photocatalyst were characterized using JEOL JSM-7800F (FESEM-EDX) at 3-5 kV with 10*k* magnification.

2.4. Photocatalytic activity

For the reaction study, around 200 mL of slurry media was irradiated with visible light source. Generally, the photocatalytic reactor consists of two parts which are a quartz cell (300 mL) with a circulating water jack and a Xe lamp (250 W) placed inside the quartz cell. The reaction temperature was kept at room temperature by using the circulating water jack. Pre-determined photocatalyst loadings, viz. 0.2, 0.5, 1.0, 1.5 and 2.0 g/L were dispersed within the 200 mL of 20 ppm MB solution in the reactor. Then, the reactor was left in the dark and rigorously stirred for 30 min to reach equilibrium. Subsequently, the reaction was exposed to the light to initiate the reaction. Around 5 mL of liquid sample was drawn every 1 h. Post-reaction, the collected samples were centrifuged and analysed. For repeatability, the experiments were repeated twice.

3. Results and Discussion

3.1. XRD analysis

Figure 1 shows the crystalline phase of the synthesized catalyst. It can be observed that the diffracted peaks are sharp. This is an indicative of a well-structured crystallite phase.

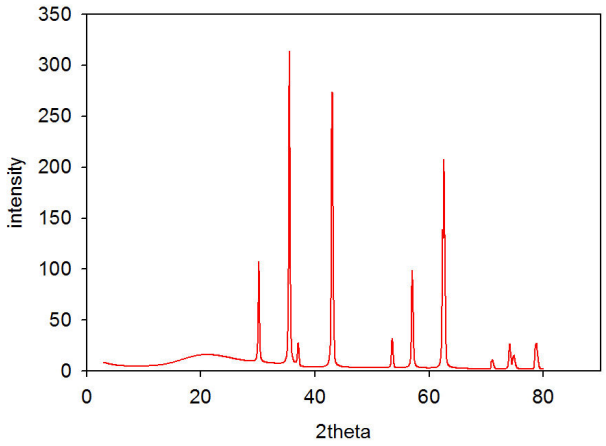

Fig. 1. XRD Pattern of $MgFe_2O_4$.

Table 1 shows the summary of the XRD results. The catalyst formulation and synthesis strategy successfully produced a new phase called magnesium ferrite or otherwise also known as the $MgFe_2O_4$ crystal. Magnesium ferrite is a member of the magnetite series of spinels with 2θ of 30.18°, 35.5°, 37.03°, 42.95°, 53.46°, 57.02° and 62.60°. In addition, the formation of cubic form of MgO was also proved by the appearance of Periclase phase at 2θ = 37.03° and 42.95°. Overall, the crystallite size ranged from 10 to 50 nm.

Table 1. Analysis of the XRD Pattern Results.

2θ (°)	Phase name	Crystallite size (nm)
30.18	Magnesioferrite (2 2 0)	43
35.51	Magnesioferrite (3 1 1)	19
37.03	Periclase (1 1 1) Magnesioferrite (2 2 2)	53
42.95	Periclase (2 0 0) Magnesioferrite (4 0 0)	11
53.46	Magnesioferrite (4 2 2)	41
57.02	Magnesioferrite (5 1 1)	34
62.60	Magnesioferrite (4 4 0)	34

3.2. FESEM-EDX analysis

Figures 2. (a) to (c) shows the FESEM image at different magnifications from 5000-50000kx. The images show that it consists of particles with diameter <100nm. Figure 2 (d) shows the EDX spectrum of $MgFe_2O_4$ at 2.061 keV which indicates that $MgFe_2O_4$ nanoparticles were mostly comprised of Mg, Fe and O elements. Oxygen element consists of 34.79 wt %, magnesium element consists of 28.77 wt % and iron consists of 36.44 wt %.

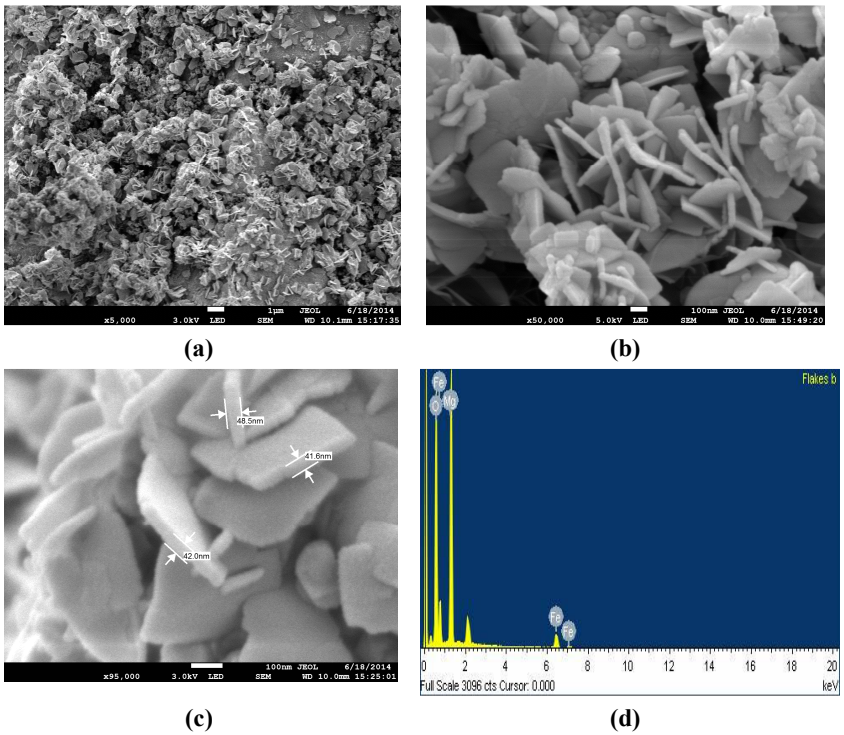

(a) **(b)**

(c) **(d)**

Fig. 2. FESEM-EDX image of the $MgFe_2O_4$.

3.3. Photocatalytic activity

3.3.1. Blank Run

In order to be sure that the MB decomposition was largely due to the photocatalytic effect and not because of the photodecomposition, blank run without the presence of $MgFe_2O_4$ was carried out and the results were compared with the 0.2 g/L of $MgFe_2O_4$. In all reactions involving the $MgFe_2O_4$ photocatalyst, the reaction media was left-stirring for 30 min to attain adsorption equilibrium before the visible light source was turned on.

Figure 3 shows the degradation patterns of 20 ppm of MB as well as its corresponding conversion, X(%). It can be observed that photodecomposition indeed took place with attainment of 40% MB degradation at the 6^{th} h. Significantly, the presence of $MgFe_2O_4$ photocatalyst has boosted the degradation rate of the MB which recorded a near-complete after 5 h of reaction time. This has confirmed that the photocatalyst employed in the current work exhibited excellent photoactivity towards the MB under the visible-light source irradiation.

In addition, the dominance of catalytic effect was only noticeable beyond 1 h of irradiation. This may be attributed to the lag time required by the system to achieve steady-state conditions.

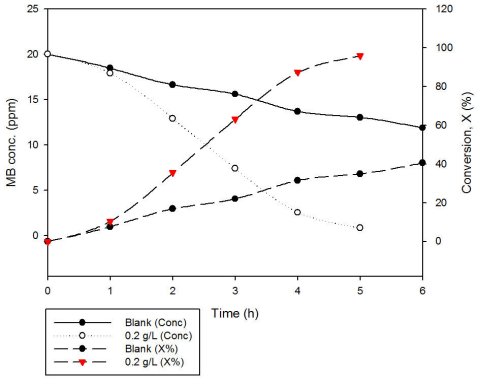

Fig. 3. Irradiation of 20 ppm MB with visible-light at 250 W.

3.3.2. Effects of photocatalyst loadings

The dosage of $MgFe_2O_4$ influences the level of MB photocatalytic degradation, i.e., if the loading is insufficient, then the decomposition rate is slow. Nevertheless, if the dosage of catalyst is excessive, then it may block the light source from penetrating into the slurry media; consequently, the MB decomposition rate will be lowered too. Therefore, the optimum loading was determined from the current work based on two separate runs and the results are presented in Fig. 4.

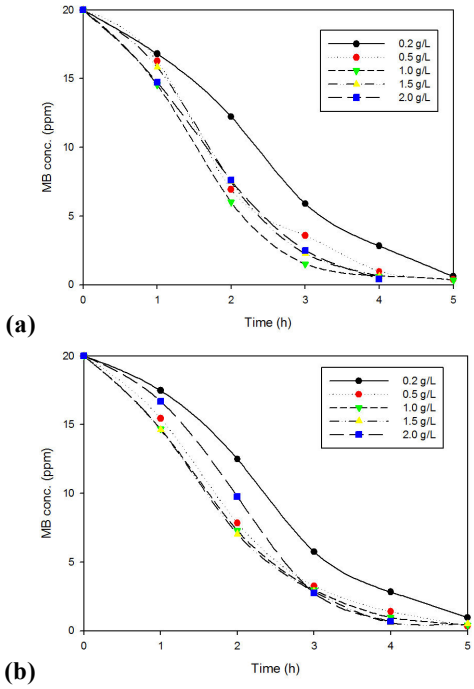

Fig. 4. Effects of Photocatalyst Loading for (a) First Run, (b) Second Run.

From the separate runs, it can be concluded that the photocatalytic decomposition trend of MB solution (20 ppm) as a function of catalyst loading was repeatable. For instance, the decomposition rate over the 0.2 g/L $MgFe_2O_4$ photocatalyst was always the slowest. It can also be seen that the loading at 1.0 g/L and 2.0 g/L of $MgFe_2O_4$, respectively, exhibited faster rate compared to the loading at 0.5 g/L of $MgFe_2O_4$ photocatalyst judging by the lower MB concentration attained at any fixed time of reaction. Indeed, both 1.0 and 1.5 g/L loadings seems to offer nearly similar photocatalytic effect. Nevertheless, beyond the loading of 1.5 g/L in particular, i.e., at 2.0 g/L of $MgFe_2O_4$ photocatalyst, the MB decomposition noticeably became lower suggesting that the optimum loading in our current work was 1.0 g/L.

The decomposition behaviour can be further described by the common Power Law model. For a batch reactor with photocatalytic kinetics behaving in *n*-order of reaction:

$$\frac{dC_A}{dt} = kC_A{}^n \tag{1}$$

Upon integrating the Eq. (1), the following equation can be produced:

$$C_A = C_{Ao} - kt \quad \text{for } n = 0 \tag{2}$$

$$\ln\left(\frac{C_{Ao}}{C_A}\right) = kt \qquad \text{for } n = 1 \tag{3}$$

$$\frac{1}{C_A} - \frac{1}{C_{Ao}} = kt \quad \text{for } n = 2 \tag{4}$$

whereby

C_{Ao} = Initial concentration (mg L^{-1}),

C_A = Concentration at time t (mg L^{-1}),

t = time (h), and

k = apparent specific reaction rate (h^{-1}).

Figure 5 shows the resulting linearization plots. It can be observed that only the power law model with n = 0 can give the best fitting compared to n = 1 and n = 2. This suggests that in our current investigation, zero-order can capture the photocatalytic kinetic decomposition trend. The attempt to model the decomposition behaviour to the first-order of reaction has returned regression coefficient, R^2 ranged from 0.80 to 0.89 indicative of non-compliance to the observed decomposition rate whilst the second-order produced poorer fitting results. For the first-order rate of reaction, however, the fitting exercises produce the kinetic parameters and regression coefficients as summarized in Table 2. The zero-order reaction as indicated by the current work implied that the decomposition was independent of the MB concentration. Practically, this may be explained by the relatively high initial concentration of MB (20 ppm), hence the independence.

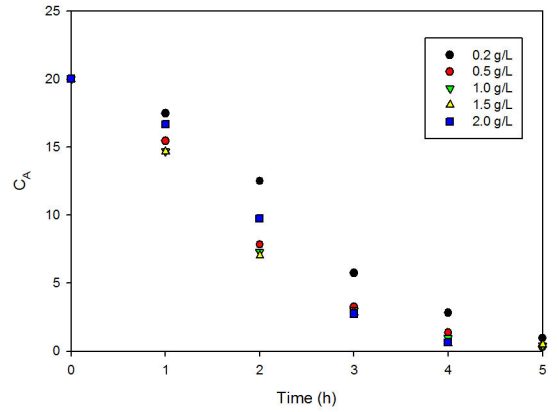

(a)

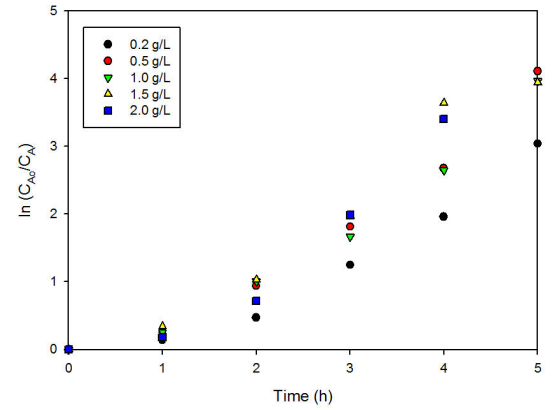

(b)

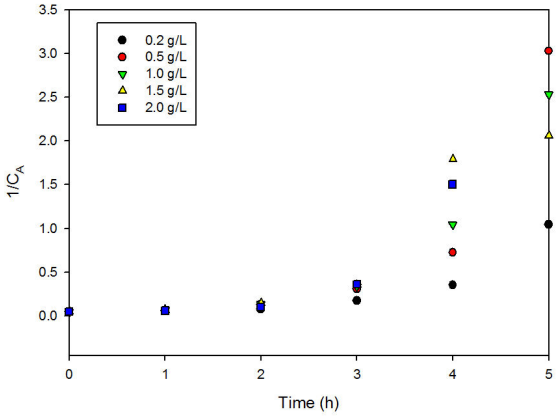

(c)

Fig. 5. Kinetics Modelling of the MB Photocatalytic Decomposition for (a) $n = 0$; (b) $n = 1$ and (c) $n = 2$.

Table 2. Kinetics parameter from the power law modelling with *n* = zero.

Catalyst loading (g/L)	k (h^{-1})	R^2
0.2	4.17	0.97
0.5	4.15	0.93
1.0	4.10	0.92
1.5	4.11	0.91
2.0	5.26	0.97

4. Conclusions

The current work successfully demonstrated that the MB aqueous solution can be degraded over the $MgFe_2O_4$ photocatalyst when the reaction was irradiated with visible range light source. The optimum loading was 1.0g/L photocatalyst.

References

1. Chala, S.; Wetchakun, K.; Phanichphant, S.; Inceesungvorn, B.; and Wetchakun, N. (2014). Enhanced visible-light-response photocatalytic degradation of methylene blue on Fe-loaded $BiVO_4$ photocatalyst. *Journal of Alloys and Compounds*, 597, 129-135.
2. Shannon, M.A.; Bohn, P.W.; Elimelech, M.; Georgiadis, J.G.; Marinas, B.J.; and Mayes, A.M. (2008). Science and technology for water purification in the coming decades. *Nature*, 452, 301-310.
3. Hoffmann, M.R.; Martin, S.T.; Choi, W.; and Bahneman, D.W. (1995). Environmental applications of semiconductor photocatalysis. *Chem. Rev.*, 95, 69-96.
4. Pourahmada, A.; Sohrabnezhad, Sh.; and Kashefian, E. (2010). AgBr/nanoAlMCM-41 visible light photocatalyst for degradation of methylene blue dye. *Spectrochimica Acta Part A*, 77, 1108-1114.
5. Vadivel, S.; Vanitha, M.; Muthukrishnaraj, A.; and Balasubramanian, N. (2014) Graphene oxide–BiOBr composite material as highly efficient photocatalyst for degradation of methylene blue and rhodamine-B dyes. *Journal of Water Process Engineering*, 1, 17–26.
6. Eng, Y.Y.; Sharma, V.K.; and Ray, A.K. (2010). Photocatalytic degradation of nonionic surfactant, Brij 35 in aqueous TiO_2 suspensions. *Chemosphere*, 79, 205-209.
7. Sharma, V.K.; Burnett, C.R.; Rivera, W.; and Joshi, V.N. (2001). Heterogeneous photocatalytic reduction of ferrate(VI) in UV-irradiated titania suspensions. *Langmuir*, 17, 4598-4601.
8. Sharma, V.K.; and Chenay, B.V.N. (2005). Heterogeneous photocatalytic reduction of Fe(VI) in UV-irradiated titania suspensions: effect of ammonia. *J. Appl. Electrochem*, 35, 775-781.
9. Sharma, V.K.; Graham, N.J.D.; Li, X.; and Yuan, B. (2010). Ferrate(VI) enhanced photocatalytic oxidation of pollutants in aqueous TiO2 suspensions. *Environ. Sci. Pollut. Res.*, 17, 453-461.

10. Casbeer, E.; Sharma, V.K.; and Li, X.Z. (2012). Synthesis and photocatalytic activity of ferrites under visible light: A review. *Journal of Separation and Purification Technology*, 87, 1-14.
11. Shahid, M.; Liu, J.; Ali, Z.; Shakir, I.; Warsi, M.F.; Parveen, R.; and Nadeem, M. (2013). Photocatalytic degradation of methylene blue on magnetically separable $MgFe_2O_4$ under visible light irradiation. *Materials Chemistry and Physics*, 139, 566-571.
12. Lee, S. (2004). Development of magnetic composite photocatalytic particles.
13. Kim, H.G.; Borse, P.H.; Jang, J.S.; Jeong, E.D.; Jung, O.S.; Suh, Y.J.; and Lee, J.S. (2009). Fabrication of $CaFe_2O_4/MgFe_2O_4$ bulk heterojuction for enhanced visibl light photocatalysis. *Chem.Commun.,* 39, 5889-5891.
14. Zhang, L.; He, Y.; Wu, Y.; and Wu, T. (2011). Photocatalytic degradation of RhB over $MgFe_2O_4/TiO_2$ composite materials. *Materials Science and Engineering B*, 176, 1497-1504.
15. Maensiri, S. (2008). Magnesium ferrite ($MgFe_2O_4$) nanostructures fabricated by electrospinning. *Nanoscale Res Letters*, 4(3), 221-228.
16. Zhao, L.; Li, X.; Zhao, Q.; Qu, Z.; Yuan, D.; Liu, S.; Hu X.; and Chen, G. (2010). Synthesis,characterization and adsorptive performance of $MgFe_2O_4$ nanospheres for SO_2 removal. *J. Hazard. Mater*, 184, 704-709.